The following are results arising from the research activities discussed in the previous section.

•Star Formation Rates in Damped Lyα Systems

I have developed a new technique based on HIRES observations that yields the heating rate of neutral gas in damped Lyα systems (DLAs), and from that the star formation rate (SFR) per unit comoving volume. Until now, comoving SFRs have been obtained for highly luminous objects such as the Lyman Break Galaxies. My technique measures rates in objects more representative of the protogalactic mass distribution and at redshifts currently inaccessible to the Lyman Break Technique.

The idea - based on the heating mechanism for the ISM - is as follows: Massive stars that form in the DLA neutral gas emit far UV radiation that illuminates dust grains known to be present in the gas. Some of the incident photon energy goes into photoejected electrons which then heat the gas. In this case, the heating rate per nucleon, $\Gamma_d \propto \kappa\epsilon J$, where κ is the dust-to-gas ratio, ϵ is the heating efficiency, and the mean intensity of far UV radiation, J, is proportional to $\dot{\psi}_*$, the SFR per unit area. Since ϵ is well determined, we can measure $\dot{\psi}_*$ provided we know κ and Γ_d. I measure Γ_d by equating it to the [C II] 158 μm cooling rate, which originates from spontaneous emission between the $^2P_{3/2}$ and $^2P_{1/2}$ fine-structure states of C II. I infer the cooling rate from the strength of the C II* λ 1335.7 absorption line, which arises from the excited $^2P_{3/2}$ state.

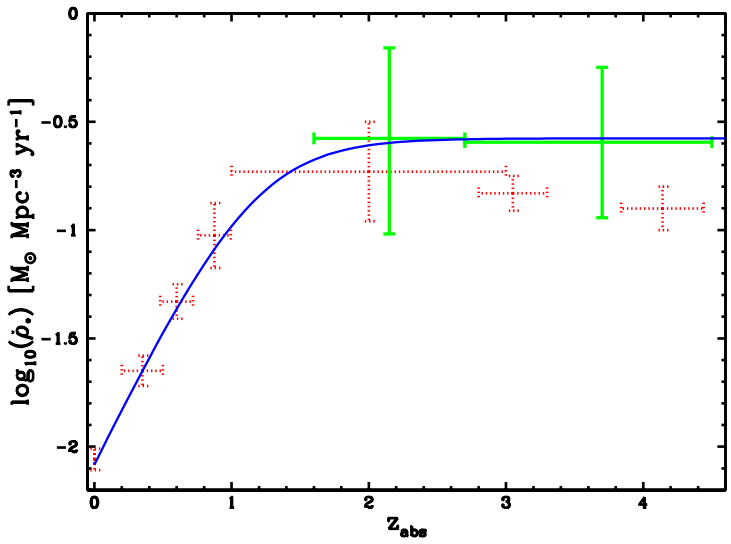

Figure 1: Star formation rate per unit comoving volume versus z for Einstein de-Sitter cosmology with $h = 0.5$. Red data points denote galaxies detected in emission. Green data points and error bars denote DLAs for the CNM solutions. Blue curves are fits to the DLA data and lower-z galaxy data.

By measuring cooling rates in about 50 DLAs and by obtaining κ from element abundance patterns I reached the following conclusions:

(1) The star formation rate per unit area is similar to that in our Galaxy ($\log\dot{\psi}_* = -2.4$ M$_\odot$ kpc^{-2} y^{-1}).

(2) At $z = 1.6$ to 4.5 the SFR per unit comoving volume, $\dot{\rho}_*(z)$, for DLAs is similar to $\dot{\rho}_*$ for Lyman Break Galaxies (see Fig. 1).

(3) C II* absorption in DLAs arises in a cold neutral medium (CNM: $T \sim 100$ K) rather than a warm neutral medium (WNM: $T \sim 8000$ K): the WNM case is ruled out because it implies much higher star formation rates, which result in background radiation with intensities that exceed observed upper limits.

(4) These results have several implications, two of which are shown in Figure 2. Specifically, Figure 2a shows evidence for a possible correlation between $\dot{\psi}_*$ and the low-ion velocity interval Δv_{low}, which may indicate that Δv_{low} is a global quantity, since $\dot{\psi}_*$ is an average over the entire DLA. In that case the velocity interval would be the virial or circular velocity, which would be a valuable diagnostic for numerical models of DLAs. Figure 2b reveals a systematic absence of low SFRs at high metal abundances, [Si/H] (where [Si/H]=$\log_{10}$(Si/H)$-\log_{10}$(Si/H)$_\odot$). This suggests that the metals we see in DLAs at the absorption redshift are produced by SFRs at that redshift rather than previous star formation histories.

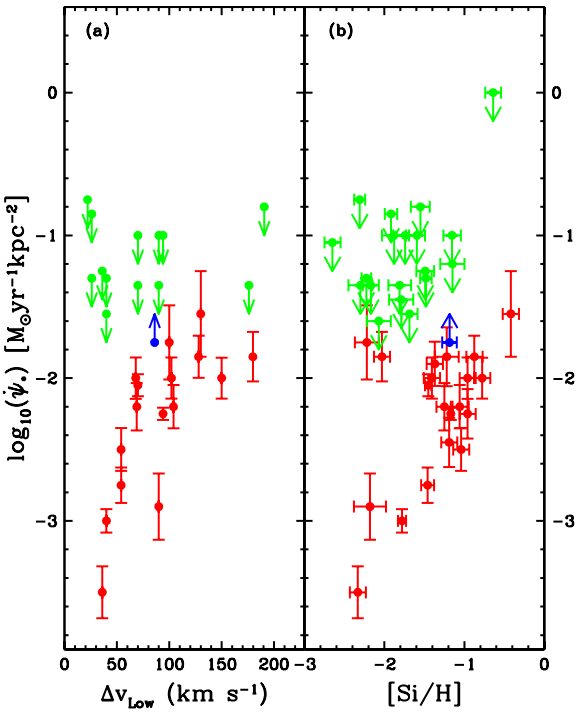

Figure 2: (a) $\dot{\psi}_*$ vs. low-ion velocity interval Δv_{Low}. Red, blue, green points are positive detections, lower, and upper limits. (b) $\dot{\psi}_*$ vs. [Si/H]. Color code same as (a)

•Metallicity Evolution

Figure 3 summarizes our most recent results on the metallicity evolution of DLAs. The data were acquired with the HIRES echelle spectrograph (red boxes) and the ESI echelette spectrograph and imager (blue boxes) on the Keck 10 m telescopes. The Figure shows the metal abundance, [M/H] (where M is Zn, Si, S or other elements undepleted by dust) versus redshift for over 100 DLAs. The size of each data point is proportional to log$N$(H I) to indicate the relative contributions to the cosmic metallicity, $< Z >$; i.e., the column density weighted mean [M/H]. We measure $< Z >$ since it equals the ratio of the comoving density of metals to that of hydrogen. The data at $z > 1.6$ are divided into 5 redshift bins containing equal numbers of DLAs. The black data points show the $< Z >$ averaged over each bin.

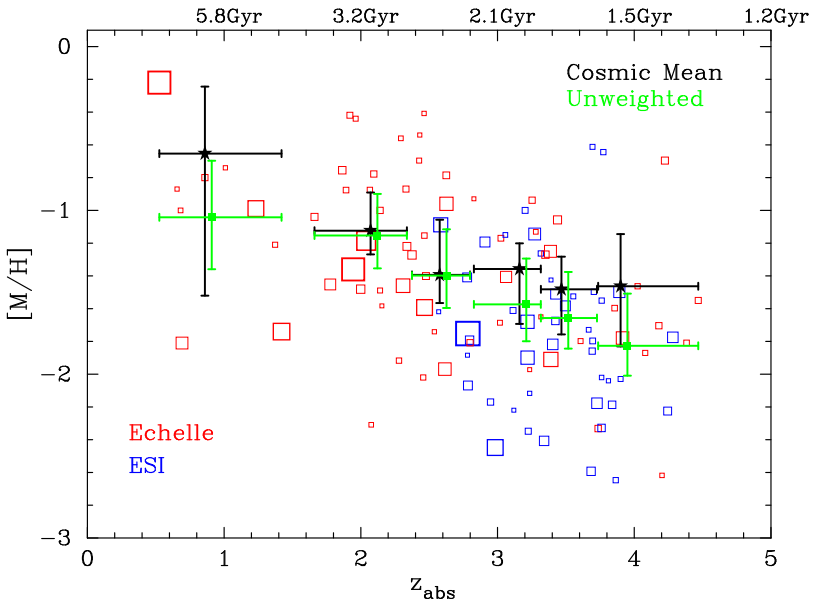

Figure 3: [M/H] vs. z. Red squares are data points taken with HIRES. Blue circles are column-density weighted mean, $< Z >$, for redshift bins discussed in text. Green points are data taken with ESI

.

The slight but statistically significant increase of $< Z >$ with decreasing redshift is the first robust evidence for metal enrichment of DLAs with time, which is predicted by models for chemical evolution. However, the increase is slower than predicted. Indeed, based on the $\dot{\rho}_*$ discussed in the previous section, $< Z >$ should be significantly higher than observed at $z \approx 2.5$. Furthermore, note that out of the 100 objects in Figure 3, none has [M/H] < -2.7. This is true even though we could have measured [M/H] $= -3.5$ in most DLAs. Whether this "floor" is a function of population III pre-enrichment is a matter for debate.

•Elemental Abundance Patterns in a Galaxy at $z = 2.626$

My colleagues and I recently obtained accurate abundances for 25 elements in a DLA with redshift z=2.626. The high metallicity of this DLA, [O/H]=−0.5, high H I column density, N(H I)= 2×10^{21} cm^{-2}, and brightness of the background quasar, B=17.7, combine to give an unprecedented look at chemical enrichment in a young galaxy. Figure 4 reveals the nucleosynthetic pattern of this galaxy, where the dotted line compares the solar abundance pattern scaled to the oxygen metallicity of this galaxy. Clearly, the galaxy's enrichment pattern resembles the Sun. On the other hand, the young age of the galaxy (<2.3 Gyr) would imply a nucleosynthetic pattern dominated by short-lived massive stars. This is supported by the enhanced abundances of the α elements (O,Mg,Si) relative to Zn, the only Fe-peak element not depleted onto dust grains known to be present in the gas. The α enhancement suggests enrichment by massive stars. Note also the decrease of [α/Zn] with increasing atomic number: this is the pattern predicted for enrichment by massive stars. Finally, all the odd-Z elements show sub-solar relative abundances marking the enhanced "odd-even" effect indicative of type II supernovae. The nearly solar Ge/O ratio raises new challenges for the production of Ge. Although the s process is expected to dominate the production of Ge, the primary s-process sight is during the "asymptotic giant branch" phase of low-mass stars, whose lifetimess may exceed the age of the universe at z=2.626.

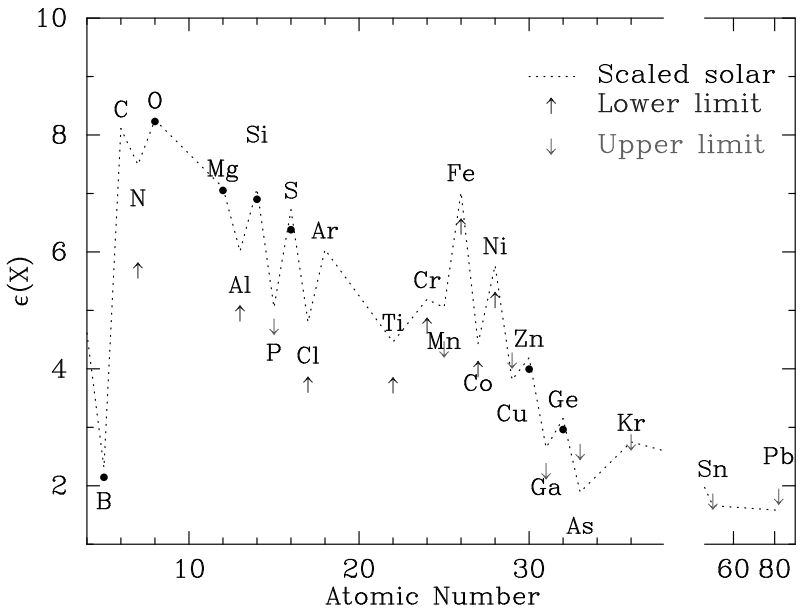

Figure 4: Nucleosynthetic enrichment pattern for the DLA toward Q0812+32. The y axis is the dust-corrected abundance on a logarithmic scale, where H is defined to have $\epsilon(X) = 12$.

Finally, the close resemblance between the abundance patterns of this DLA and of massive early-type galaxies leads us to speculate that this is a young early-type galaxy. In fact, in many respects this DLA resembles another high-z population, the "Lyman-Break" galaxies, which are detected in emission, and which are also thought to be the progenitors of massive early-type galaxies. We plan to search for starlight emitted by this DLA.

•Kinematics of DLAs

We have studied the kinematics of the neutral and ionized gas in DLAs by obtaining accurate HIRES velocity profiles of low ions such as Fe II and high ions such as C IV. The results of our work are summarized in Figure 5. This compares the low-ion and high-ion velocity profiles. Our statistical analysis supports the visual impression that the ionized gas and the neutral gas comprise distinct kinematic subsystems. This is indicated by the misalignment in velocity space of the narrow components that make up the velocity profiles, and the difference between the widths of the velocity profiles. However, despite their differences, the kinematic subsystems are interrelated as indicated by a statistically significant C IV versus low-ion cross-correlation function. Moreover, the velocity intervals of the C IV profiles exceed those of the the low-ions in 29 out of 32 cases. This indicates the two systems are in the same gravitational potential well.

We have used these results to test the standard scenario in which the high-ion (ionized) gas undergoes radial infall into dark matter halos containing centrally located rotating disks comprising the low-ion (neutral) gas. Neither the CDM nor passive evolution models predict kinematics that are consistent with all our kinematic tests. The main problem is that the models fail to reproduce the significant amplitude of the C IV versus low-ion cross-correlation function. We are currently testing new models in which the infalling ionized gas has the same angular momentum per unit mass as the collapsed neutral gas. In principle this should increase the correlation between the velocity fields of the two components.

The origin of the velocity fields in DLAs remains an unsolved problem. The evidence in

Figure 2a suggests the motions are related to the depth of the gravitational potential well

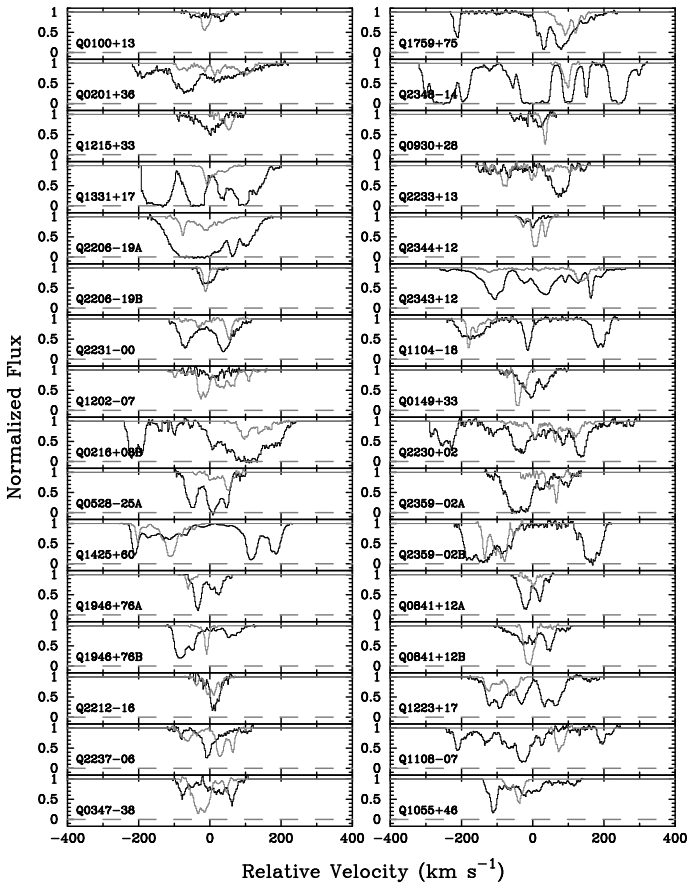

Figure 5: Velocity profiles of high-ions (dark lines) and low ions (light lines) in 32 separate DLAs

into which gas in DLAs has settled. On the other hand, we have just seen that no realistic model has yet been constructed to explain the strong correlation between the velocities of the neutral and ionized gas. The recent detection of a galaxy associated with the z=1.92 DLA toward Q2206−19 provides spatial information not available previously, which will constrain the range of kinematic solutions in a DLA for the first time.

•Survey for Lyman-Break Galaxies Correlated with DLAs

Graduate student Jeff Cooke is searching for a cross-correlation between Lyman Break Galaxies (LBGs) and DLAs. LBGs are widely believed to be the massive progenitors of modern early type galaxies. The strong clustering they exhibit at $z \sim 3$ can be explained in terms of biassing; i.e., massive galaxies preferentially form in clusters at high redshifts. If DLAs have similar masses, they should exhibit a significant cross-correlation amplitude with the LGBs. Since the masses of DLAs are highly controversial, but of considerable value for theories of galaxy formation, any information would be worthwhile.

To that end, graduate student Jeff Cooke has used the Keck telescopes to image 9 fields centered on quasars with foreground DLAs with $z \sim 3$. All 9 fields have been imaged in 5

bands ($u'BVRI$) to 1σ magnitude depths of ≥ 28.5 in $u'BVR$ and ≥ 27.5 in I. Photometry has been performed on 17,343 objects detected in all fields. Photometric selection, using the Lyman-break technique, resulted in the detection of 985 LBG candidates in 9 fields. The photometry was followed up with narrow-band spectroscopy using LRIS and DEIMOS multi-slit spectrographs. Spectra of 600 candidates was obtained yielding 300 confirmed LBGs. The spectra of one of these is shown in Figure 6.

To determine the DLA-LBG cross-correlation function properly, more than 300 LBGs are needed to correlate with the 10 DLAs in 9 fields. Preliminary results show (1) significant clustering in some fields, and (2) that the number of LBGs associated with DLAs exceeds the null hypothesis of no cross-correlations. But the analysis is just beginning.

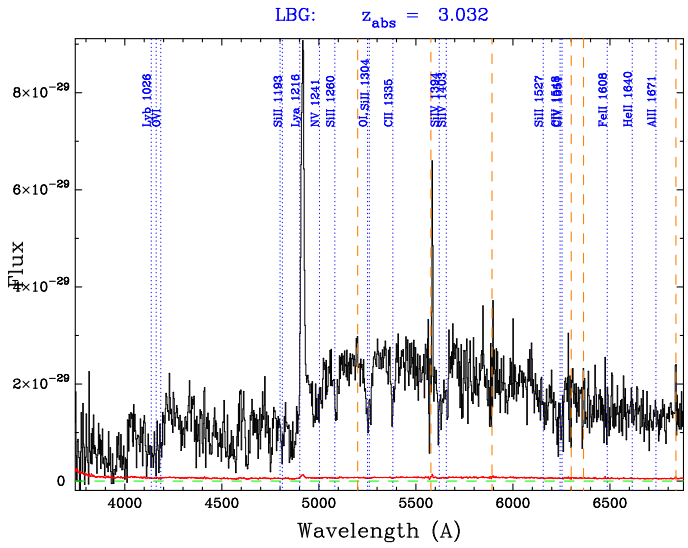

Figure 6: Spectrum of a Lyman Break Galaxy from $z \sim 3$ multi-slit data. Expected meal absorption-emission features marked with dotted lines and sky emission lines marked with dashed lines. This LBG exhibits stron Lyα emission, which is observed in about 25 % of all LBGs. Flux decrement blueward of Lyα emission due to absorption in Lyα forest

•Possible Detection of Cosmological Evolution of the Fine Structure Constant

Using high-resolution spectra of metal lines obtained with the Keck I HIRES spectrograph my collaborators and I have searched for time variability of the fine structure constant, α ($=e^2/\hbar c$). Variations in α would lead to detectable shifts in the rest wavelengths of redshifted UV resonance lines such as those used to deduce kinematics and metallicities in DLAs (e.g. Ni II, Cr II, Zn II, etc). For relativistic fine structure splitting in alkalai-type doublets, the separation between the lines is proportional to α^2, so that small relative variations in the separation are proportional to α. We used a new technique which is more sensitive than the alkalai technique, since it is not restricted to transitions with respect to the same ground state. Rather it compares transitions relative to different ground states in different species. Using species with widely differing atomic masses produces an increase in sensitivity because the difference between ground-state relativistic correction can be large and of opposite sign. We measure variations in α, i.e. $\Delta\alpha/\alpha=(\alpha_z/\alpha) - 1$, by explicitly including these variations in a Gauss-Newton optimization code in which other parameters such as velocity width and thermal width of the absorption lines are allowed to vary freely. The results based on 72 quasar absorption systems are summarized in Figure 7. The figure shows possible evidence

that $\Delta\alpha/\alpha$ decreases with z.

This potentially exciting result has recently been checked with independent data sets, and so far has not been confirmed. However, the statistical significance of the new results is such that they are not formally inconsistent with our results. We are using the Keck HIRES spectrograph to detect the predicted variations, $\Delta\alpha/\alpha = -(0.62\pm0.10)\times10^{-5}$, in a single DLA using the molecular iodine cell simultaneously with the quasar spectrum. The iodine cell superimposes several narrow absorption lines per Å between 4950 and 5900 Å. Thus wavelength errors caused by atmospheric dispersion, guiding errors on the slit, and changes in optics are all shared by the iodine cell and quasar spectrum. We have already shown this technique reduces wavelength errors dramatically. We expect to detect the predicted 140 m/s relative shift of Fe II 1608 and Fe II 1611 lines at 3-σ significance.

•Thick Disk Abundance Patterns

We (Prochaska et al. 2000) have obtained accurate HIRES spectra for 10 thick disk stars. Our analysis confirms previous studies of O and Mg which show enhancements of [O/Fe] and [Mg/O] relative to the thin disk. We also find that the elements Si, Ca, Ti, Mn, Co, V, Zn,Al, and Eu have a chemical history distinct from the thin disk. Moreover, the thick disk

Results

Sample at present:

28 MgII/FeII absorption systems towards 17 QSOs (Churchill)

18 DLA absorption systems (+ 3 further Mg/Fe systems) towards 13 QSOs (Prochaska/Wolfe)

21 SiIV doublets towards 13 QSOs (Prochaska/Wolfe)

All Keck spectra, <s/n> ~ 30/pixel, resolution FWHM ~7 km/s for whole dataset

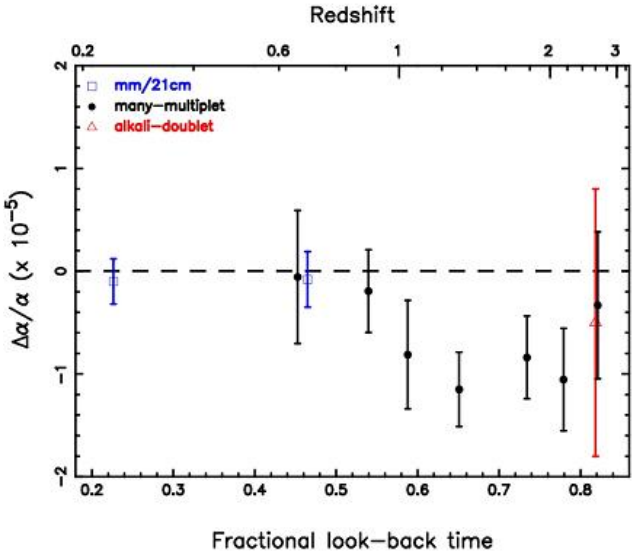

Sample	Method	N_{abs}	Redshift	$\Delta\alpha/\alpha$
FeII/MgII	MM	28	$0.5 < z < 1.8$	-0.70 ± 0.23
NiII/CrII/ZnII	MM	21	$1.8 < z < 3.5$	-0.76 ± 0.28
SiIV	AD	21	$2.0 < z < 3.0$	-0.5 ± 1.3
21cm/mm	radio	2	0.25, 0.68	-0.10 ± 0.17

TABLE I: Summary of results for 4 independent samples. Values of $\Delta\alpha/\alpha$ weighted means and are in units of 10^{-5}. MM and AD indicate "many-multiplet" and "alkali-doublet". N_{abs} is the number of absorption systems in each sample.

Overall deviation from zero is 4 sigma, (uncorrected for any systematic effects)

Figure 7: Summary of evidence for variations in α from Webb et al. (2001).

abundance patterns tend toward the values observed for halo stars with [Fe/H] = −1. This suggests that the thick disk stars had a chemical enrichment history similar to the metal-rich halo stars.

Furthermore, we find that (1) all 10 stars exhibit enhanced α/Fe ratios with O, Si, and Ca exhibiting trends of decreasing overabundance with increasing [Fe/H]. If these trends are explained by the onset of Type Ia Sn, then the thick stars formed over the course of $\geq$ 1Gyr. This slow formation time is apparently incompatible with dissipational collapse scenarios for the formation of the thick disk. Models with heating of an initially thin disk are favored instead.

Figure 8 shows the impact of the thick disk abundances on interpretations of abundances in DLAs. The DLA abundance pattern exhibits a classic example of halo abundances with enhanced α-elements and deficient Mn and normal Ni,Cr, and Al. While the [Zn/Fe] ratio of DLAs is high, the overall type II Sn pattern is clearly evident. In fact there is tentative evidence for an evolutionary sequence in the abundances of DLAs to the thick disk stars.

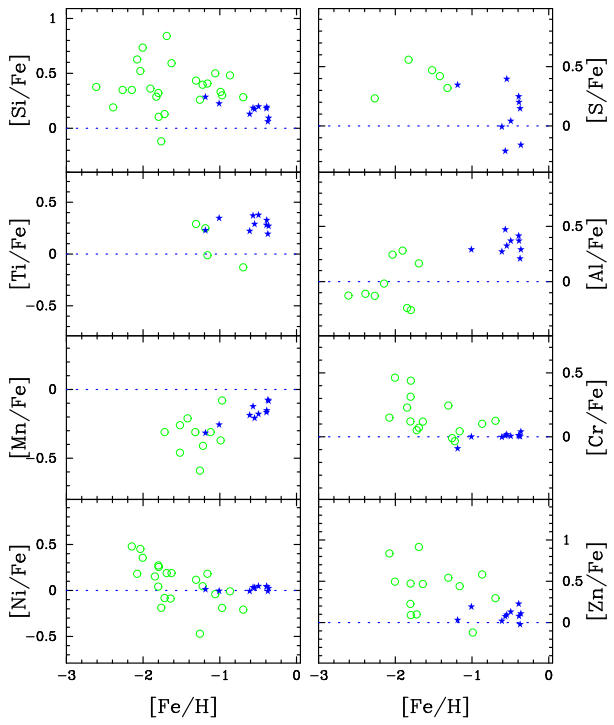

Figure 8: Comparison of abundance patterns of DLAs (green circles) and thick-disk stars (blue stars) from Prochaska et al. (2000).

On the other hand, the abundance pattern is also consistent with element depletion in the ISM. This would explain the enhanced Si, Zn, and S, but is inconsistent with the Mn trend. Our guess is that the DLAs consist of a type II Sn pattern on top of a small amount of dust.